Organic Electronics 12 (2011) 1927–1935

Contents lists available at SciVerse ScienceDirect

Organic Electronics

journal homepage: www.elsevier.com/locate/orgel

Outcoupling of trapped optical modes in organic light-emitting devices with one-step fabricated periodic corrugation by laser ablation

Yu Bai [a], Jing Feng [a,*], Yue-Feng Liu [a], Jun-Feng Song [a], Janne Simonen [b], Yu Jin [a], Qi-Dai Chen [a], Jian Zi [c], Hong-Bo Sun [a,d,*]

[a] State Key Laboratory on Integrated Optoelectronics, College of Electronic Science and Engineering, Jilin University, 2699 Qianjin Street, Changchun 130012, People's Republic of China
[b] Optoelectronics Research Centre, Tampere University of Technology, P.O. Box 692, FIN-33101 Tampere, Finland
[c] Surface Physics Laboratory and Department of Physics, Fudan University, Shanghai 200433, People's Republic of China
[d] College of Physics, Jilin University, 119 Jiefang Road, Changchun 130023, People's Republic of China

ARTICLE INFO

Article history:
Received 23 June 2011
Received in revised form 22 July 2011
Accepted 5 August 2011
Available online 27 August 2011

Keywords:
Organic light-emitting devices
Waveguide modes
Surface-plasmon polaritons
Laser ablation
Periodic corrugation

ABSTRACT

Introduction of microstructures into an organic light-emitting device (OLED) is being considered as an effective approach to outcouple photons trapped in waveguide (WG) and surface plasmon-polariton (SPP) modes within the devices. However, the attempt has been hampered by the difficulty in applying lithographic patterning technologies on organic materials. Here, we show the end has been simply reached by one-step directly laser ablating the hole-transporting layer of the OLEDs without inducing any optical or electrical deterioration. Three times efficiency enhancement has been experimentally attained from the corrugated OLEDs, which has then been ascribed by numerical simulation to the efficient outcoupling of the SPP and WG modes to radiation.

1. Introduction

High efficiency is one of key issues for applications of organic light-emitting devices (OLEDs) in display and lighting, for which much effort has been devoted to developing novel materials and device structures [1,2]. It is well known that the majority of the generated light is trapped in OLEDs, and it is the area in which there is still the greatest scope for significant improvements in efficiency [3]. Around 80% of internally generated light is trapped in form of waveguide (WG) modes in organic and indium-tin-oxide (ITO) anode layers, and in surface plasmon-polariton (SPP) modes associated with the metallic cathode/organic interface [4,5]. The overall power lost even reaches to ~95% for the inorganic LEDs due to higher refractive index of inorganic semiconductors [6,7]. Among various techniques to improve the light extraction [8–14], employing microstructure in the devices has exhibited its remarkable effect through controlling light output by Bragg scattering [4,12–14]. Microstructures with wavelength to subwavelength-scale periodicity has played an important role in optical and optoelectronic devices, particularly in optical fibers, distributed feedback lasers, LEDs and solar cells through manipulating the generation and propagation of photons in materials [15–17]. Introducing a microstructure onto the metallic electrode is especially crucial for recovering the power lost to the associated SPP modes by providing an additional momentum to couple the SPP modes into light [18–21]. Various lithography-based technologies are effective in introducing microstructure into LEDs due to the high physical and chemical stability of the inorganic

* Corresponding authors. Address: State Key Laboratory on Integrated Optoelectronics, College of Electronic Science and Engineering, Jilin University, 2699 Qianjin Street, Changchun 130012, People's Republic of China (J. Feng and H.-B. Sun).
E-mail addresses: jingfeng@jlu.edu.cn (J. Feng), hbsun@jlu.edu.cn (H.-B. Sun).

1566-1199/$ - see front matter © 2011 Elsevier B.V. All rights reserved.
doi:10.1016/j.orgel.2011.08.004

semiconductors. However, these approaches are difficult to apply to OLEDs because organic materials are generally soluble in the solvents used in lithography, and they experience optical and/or electrical deterioration when exposed to water, oxygen or high-energy electrons.

In order to avoid the degradation of the OLEDs, microstructuring has to start from the substrate, so that corrugation transmits through the organic layer to the opposite electrode. Periodic corrugation [22] on silica substrates by holographic lithography followed with RIE (reactive-ion etching) dry etching, and spontaneously formed quasi-periodic structure on glass substrate [23,24] have been reported. Although trapped optical modes were found coupled out, the substrate pattern transmission approach is encountered with problems such as electronic degradation since the ITO anode has to be sputtered on the corrugated substrates, which increase its surface roughness. It is obvious that the problem may be solved if microstructures are induced into a certain organic functional layer without affecting the flatness of the ITO film. Efforts have been paid along this line, for example, micromoulding [25,26] dendrimers above the ITO anode [27,28]. However, the complexity of the fabrication process and the high fluidity requirement to the polymer limits the practical application of the technology. Periodic change of the refractive index has been inscribed in the active materials without surface-relief structure in the OLEDs by holographic setup, and output characteristics of the OLEDs have been modified [29]. However, this method is restricted by realizing a polymer with both photosensitive and charge-transporting qualities to undergo a photoisomerization and act as functional layer in OLEDs. In addition, a necessity of large difference in the periodic changed refractive index for the highly efficient Bragg scattering is another limitation.

In this communication, we solve this problem by employing a one-step fabrication approach to introduce a

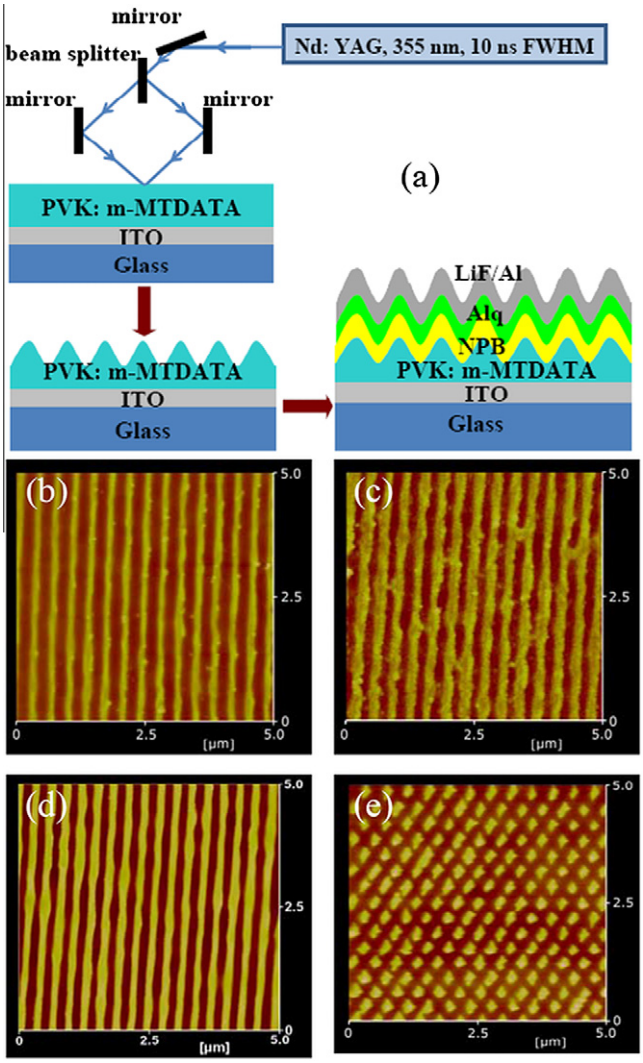

Fig. 1. Scheme of introducing periodic corrugation into OLED by laser ablation (a), and AFM images of the ablated corrugation. 1-D grating with period of 350 nm on the HTL (b) and the cathode surface of the OLED (c), the 1-D grating with period of 250 nm (d) and 2-D grating with 350-nm period on the HTL surface (e).

grating onto the functional layers of the OLEDs. Most polymers show a strong sensitivity to UV laser ablation condition and possess low ablation thresholds, so that a periodic grating can be directly recorded on the hole-transport layer (HTL) of OLEDs via laser ablation by two interference beams. Gratings with appropriate period and depth for Bragg scattering in OLEDs are easily obtained by adjusting the angle of the two beams and the laser fluence. Experimentally, three times enhancement in the current efficiency has been observed from the corrugated OLEDs with appropriate grating period. Theoretical simulations demonstrate that the power lost to both WG and SPP modes have been recovered. This one-step laser ablation on HTL provides a simple and facile approach with high resolution, high controllability and reproducibility to obtain periodically corrugated OLEDs.

2. Experimental details

2.1. Preparation of periodic microstructure by laser ablation

A conducting polymer widely used in polymer LEDs as a hole-transport material, poly(*N*-vinyl carbazole) (PVK) is chosen and it is spin-coated on the ITO glass for the fabrication of the corrugated HTL in OLEDs. 4,4′,4″-Tris(3-methylphenylphe-nylamino)triphenylamine (*m*-MTDATA) [30] was doped into the PVK with a concentration of 10% by weight to enhance the hole injection and transport of the HTL. The experimental scheme for laser ablation on PVK:*m*-MTDATA film and fabrication sequence of the corrugated OLED is illustrated in Fig. 1(a). The ablation experiments used a frequency-tripled Nd:YAG laser (Spectra-physics Company) with 3 nm pulse width, 10 ns pulse length, 10 Hz repetition rate and 355 nm wavelength. An ITO coated glass substrate was cleaned with acetone and ethanol. The HTL was spin-coated at 4000 rpm/s speed for 70 nm thicknesses. The sample was prebaked in vacuum for 30 min at 60 °C to evaporate the organic solvent. Then, the sample was exposed by two beams which were split from the UV laser with beam size of ~6 mm in diameter. The microstructure recorded on the polymer film with different period and depth was obtained by adjusting the writing angle and the laser power. The microstructure fabrication was conducted in air at room temperature using single laser pulse. The morphologies of the microstructure were characterized by an atomic force microscopy (AFM, Digital Instruments Nanoscope IIIA) in the contact mode and field emission scanning electron microscope (SEM, JSM-7500F, JEOL).

2.2. OLED fabrication and evaluation

Prepared ITO substrates coated with corrugated HTL were immediately brought into a thermal evaporation chamber. The 20 nm thick hole transporting layer of *N*,*N*′-diphenyl-*N*,*N*′-bis(1,1′-biphenyl)-4,4′-diamine (NPB), 50 nm thick emitting layer of tris-(8-hydroxyquinoline) aluminum (Alq_3) and cathode of LiF (1 nm)/Al (100 nm) were evaporated sequentially. Here, all layers were prepared by thermal evaporation in a high vacuum system with the pressure of less than 5×10^{-4} Pa. The active area of the devices was 2×2 mm^2. Their current density–voltage–luminance (*J*–*V*–*L*) characteristics were measured by Keithley 2400 programmable voltage–current source and Photo Research PR-655 spectrophotometer. The emission spectra at different observation angle were collected with a lens and then collimated and focused into the entrance slit of a 300-mm monochromator/spectrograph (SR-3031-A, Andor) to limit the angular acceptance to ~1°. The spectrogram of the emission was recorded using a charge coupled device (iDus, Andor). The OLEDs were placed on a rotation stage with the grooves parallel to the rotation axis. All of the measurements were conducted in air at room temperature.

3. Results and discussion

3.1. Investigation of periodically corrugated HTL by laser ablation

Laser ablation has been extensively studied, both theoretically and experimentally [31–33]. Several models have been proposed for ablation of polymers, involving photochemical effects (direct bond breaking) [34], photothermal effects (thermally broken bonds) [35], photophysical (mechanical stress) [36] or a combination of them. Although the chemical nature of the reaction that are involved is still not clearly verified, it does offer an alternative, simple and fast technique of direct generation of the microstructure on organic functional materials. Through combining with a multi-beam interference, the one-step fabrication of the microstructure can be faster and highly reproducible with the period from microns to sub 100 nm [37–39]. Shown in Fig. 1(b)–(e) is the atom force microscopy (AFM) images of a laser ablated grating on the PVK:*m*-MTDATA film and the cathode surfaces after deposition of organic and metallic cathode layers by thermal evaporation. As can be seen, the profile of the top surface was essentially a replication of the underlying nanostructure, therefore, forming a periodic corrugation throughout all the layers on the ITO substrate.

Due to the scattering and diffraction of the grating, the structured surface shows varied colors from structures of different periods, which are clearly observed by the naked human eyes as shown in Fig. 2(a). The microstructure on the PVK:*m*-MTDATA film in a large scale is investigated by scanning electron microscope (SEM) and shows homogeneous profile (the inset of Fig. 2(b). A 6-mm diameter area of uniform corrugation was produced with single-shot laser exposure, in another word, the exposure duration is only 10 ns. Provided that the laser pulse energy is sufficient after laser beam expansion, and assumed the laser repetition rate of 10 Hz, and the wafer transferring time of 0.1 s in a production line, the introduction of the microstructures in an entire wafer by single-pulse exposure takes only 0.1 s and as a result, the cost would be very low.

The controllability of the microstructure parameters is quite high. Experimentally, we found the groove depth is fully determined by the laser fluence at low laser energy

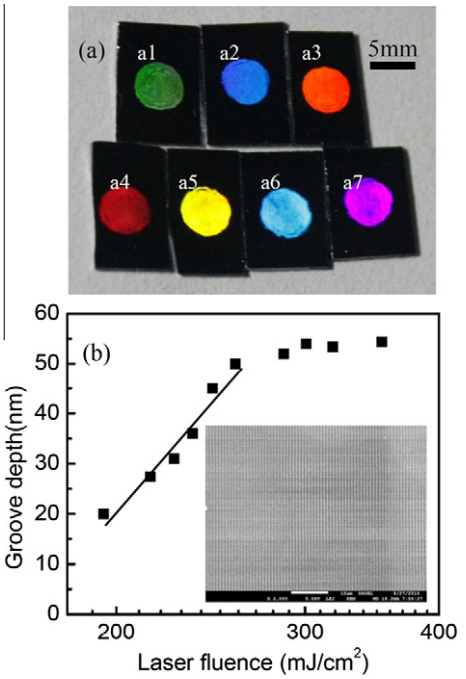

Fig. 2. (a) Photograph of the periodic corrugation on the PVK:*m*-MTDATA film with various period of a1 2000 nm, a2 1500 nm, a3 1000 nm, a4 800 nm, a5 600 nm, a6 400 nm, and a7 350 nm. (b) Etch depth by one-pulse laser ablation as a function of the laser fluence for 70 nm PVK:*m*-MTDATA film. The inset in (b) shows the large-scale SEM image of the grating on the PVK:*m*-MTDATA film with period of 800 nm and the scale bar represents 10 μm.

density (<270 mJ/cm^2), and it follows Beer's law [31], which sums up the light energy absorbed by the layer:

$$x_f = (1/\alpha)\ln(F/F_0) \quad (1)$$

where, x_f is the ablation depth per pulse. Other symbols denote: α, the linear absorption coefficient; F, the laser fluence, and F_0, the fluence threshold. The linear dependence of the ablation depth on the logarithm of the fluence is shown in Fig. 2(b), which is deviated, and is gradually saturated to ~55 nm after $F > 270$ mJ/cm^2. This derivation at high fluence is due to limitation of the ablation depth by the film thickness. The threshold fluence for the ablation of the two-beam interference on a 70-nm thick PVK:*m*-MTDATA film is $F_0 = \sim 180$ mJ/cm^2 (1.8×10^{11} W/m^2). This level of the laser irradiation, almost four-order lower than the laser-induced damage threshold of typical transparent solids, for example, 10^{15} W/m^2 for most fused silica [40], induce no any damage to the ITO substrate.

3.2. EL performance of the corrugated OLEDs

The tris-(8-hydroxyquinoline) aluminum (Alq_3)-based OLEDs with one-dimensional (1-D) periodic corrugation were fabricated according to the design in Fig. 1(a). Various grating period from 200 to 400 nm have been tested, and the grating depth is fixed at 40 nm. The devices structure is ITO/PVK:*m*-MTDATA (70 nm)/NPB (20 nm)/Alq_3 (50 nm)/LiF (1 nm)/Al (100 nm). To investigate the effect

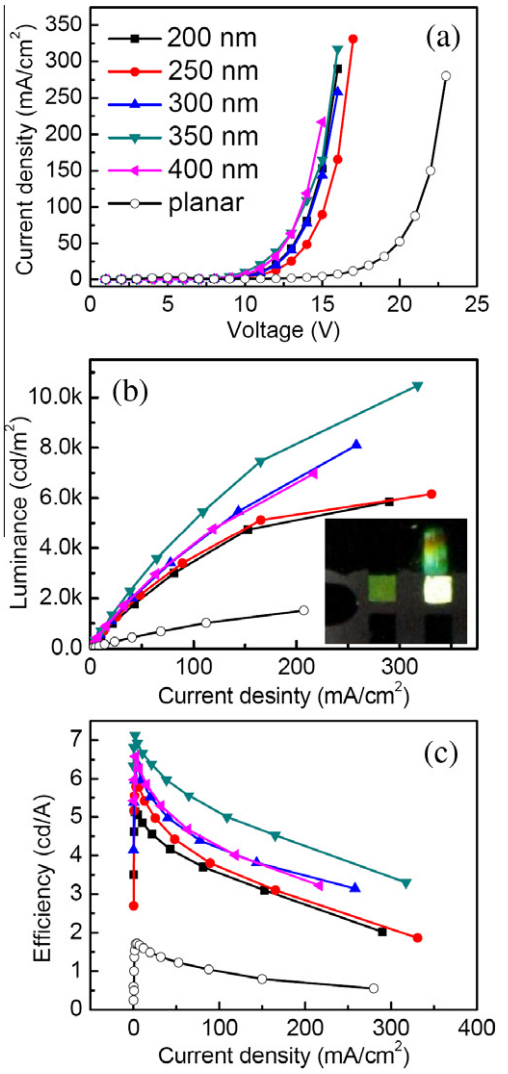

Fig. 3. EL performance of the corrugated and planar OLEDs. Current density–voltage (a), current density–luminance (b), current density–efficiency (c) characteristics. Inset in (b) shows the photograph of the operating corrugated and planar OLEDs at the same substrate and under same driving voltage.

of the grating, flat OLEDs were fabricated on the planar region of the ITO glass substrate. Considering that the average thickness of the corrugated HTL is decreased from 70 to 50 nm after laser ablation, the thickness of the HTL for the planar devices is designed to 50 nm to be equal to that of the corrugated HTL, so that the effect of the HTL thickness on the hole transport could be excluded. Actually, a 20-nm average difference between the HTL thickness before and after ablation has no much effect on the planar OLED performance through the comparison with experiment. The corrugated OLEDs show increased current density as shown in Fig. 3(a). The introduction of the corrugation has the effect on increasing the effective area of the operating devices, which would result in the increased current density. On the other hand, the ablation on the HTL has probably influenced the hole-transport

ability of the material, for which further study is needed. It can be clearly seen in Fig. 3(b) and (c) that the corrugated OLEDs exhibit much higher luminance and current efficiency than that of the planar devices and shows grating-period dependence. Both luminance and efficiency increase with the increasing grating period, and reach the maximum at 350 nm, and then decrease with further increment to 400 nm. In case of 350 nm, the luminance at the current density of 100 mA/cm^2 is 5100 cd/m^2 and the maximum current efficiency is 7.2 cd/A, respectively, while it is 910 cd/m^2, and 1.8 cd/A, respectively, for the planar devices. This corresponds to three times enhancement in the maximum current efficiency. The photograph of the operating OLEDs at the same substrate and under same driving voltage of 12 V (inset in Fig. 3(b)) indicates that much brighter emission can be obtained from the corrugated OLED.

3.3. EL spectra from the corrugated OLEDs

Understanding of the enhancement mechanism starts from analyzing the scattering of guided modes from a device by measuring its emission spectra as a function of observation angle. The scattered modes appear as additional emission peaks in intensity which shifts in wavelength as the angle varies. Fig. 4 shows the electroluminescent (EL) spectra measured from the experimental devices employing different grating period at several observation angles off to the surface normal. The EL spectra from the corrugated devices are more complex than that from the flat devices. Additional peaks with different wavelength are observed from the devices with varied grating period. The EL spectra at normal direction from the devices with different grating periods are summarized in Fig. 4(f) together with an EL spectrum from a planar

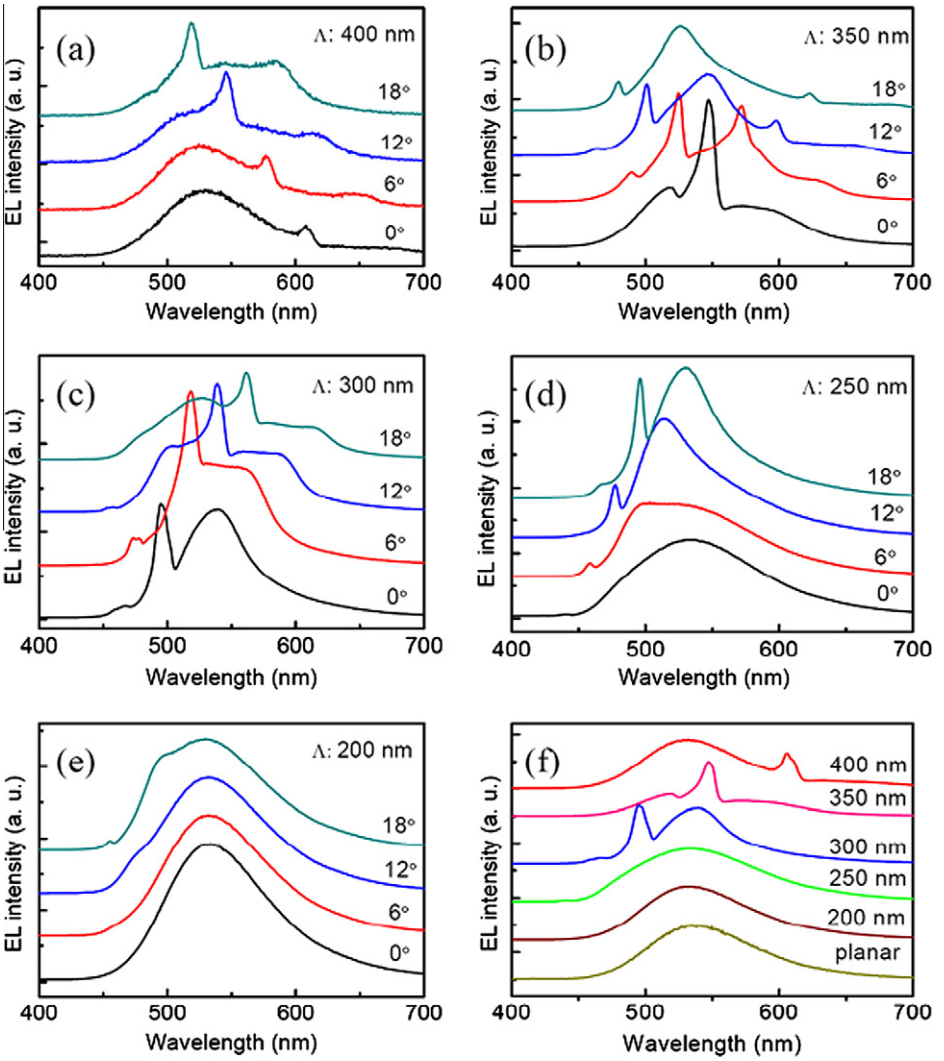

Fig. 4. The EL spectra at different observation angle from the corrugated OLEDs with various grating period (Λ). (a) 400 nm, (b) 350 nm, (c) 300 nm, (d) 250 nm, and (e) 200 nm. Their EL spectra at normal direction are summarized in (f).

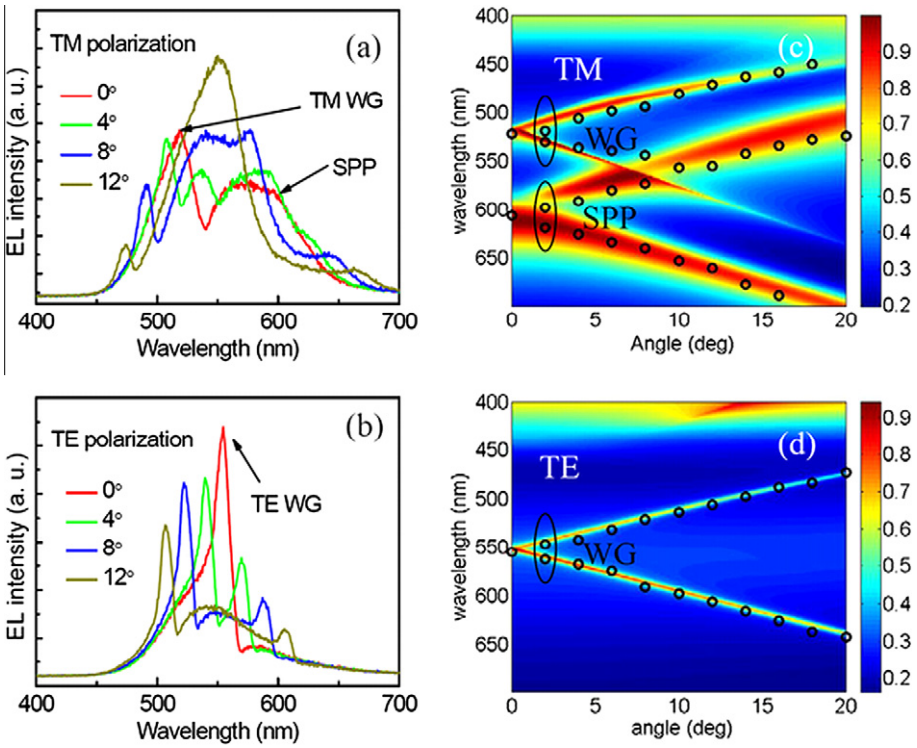

Fig. 5. Measured EL spectra with TM (a) and TE (b) polarization at different observation angle from the corrugated OLEDs with 350-nm grating. And the wavelength versus incident angle for the calculated dispersion relation of the corrugated OLEDs for TM (c) and TE (d) polarization. The measured dispersion relation extracted from the EL spectra (circles) is also shown in (c) and (d).

device at normal direction. All the additional peaks exhibit obvious blueshift with the decreasing grating period, and some of them then move out of the EL spectra for the grating period less than 250 nm. For the devices with 350 nm grating period, peaks at around 520, 547 and 595 nm are observed at normal direction, and the bandwidth of the peak at 595 nm is broader than that of the others. Each of them splits into two peaks, which shifts in wavelength with the increasing observation angle. Both TM and TE polarized EL spectra are also measured and shown in Fig. 5(a) and (b), which indicate that the modes corresponds to the emission peaks of 520 and 595 nm at the normal direction are TM polarized and that of 547 nm are TE polarized.

4. Simulated optical modes in the corrugated OLEDs

To establish the optical modes supported by the microstructured OLEDs, absorption spectra are simulated. A number of absorption maxima could be seen, if the incident light is coupled into modes supported by the structure. We apply the scattered matrix approach [41] to deal with our periodically microstructured OLED with metal and organic multilayered structure. The overall scattering of the OLEDs is determined by first evaluating a matrix of scattering parameters for each individual layer through the solving of Maxwell's equation, and then forming a scattering matrix for the entire structure by the relevant boundary conditions. As high as fifty orders spatial harmonics are taken into consideration. Given an incoming wave from the ITO glass side, the reflection waves have been computed. Absorption spectra are obtained from complementary relation between reflection and absorption. The grating with rectangular cross section and fill factor of 50% was employed and the refractive index of the organic materials employed in the OLEDs was measured by ellipsometry for the simulation. The dispersion map derived from the simulated absorption spectra for the corrugated device with 350 nm grating period and for both TM and TE polarization is shown in Fig. 5(c) and (d), in which the absorption intensity appears as a function of both incident angles and absorption wavelength. The dispersion relation curve constructed from the experimental EL emission spectra with both TM and TE polarization (Fig. 5(c) and (d)) are also plotted. It can be seen that there is excellent agreement between the theoretical calculation and experimental measurement. Actually both the calculated peak position at different angle and bandwidth of the emission spectra coincide with that of measured data very well. The optical modes within the device structure appear as EL maxima indicates an efficiently outcoupling of light from those optical modes, which are normally non-radiative, by the addition of the appropriate wavelength scale microstructure.

Both SPP and WG modes could be coupled out by the microstructure. The spatial magnetic field (H_y) distribution across the device structure as a function of position with

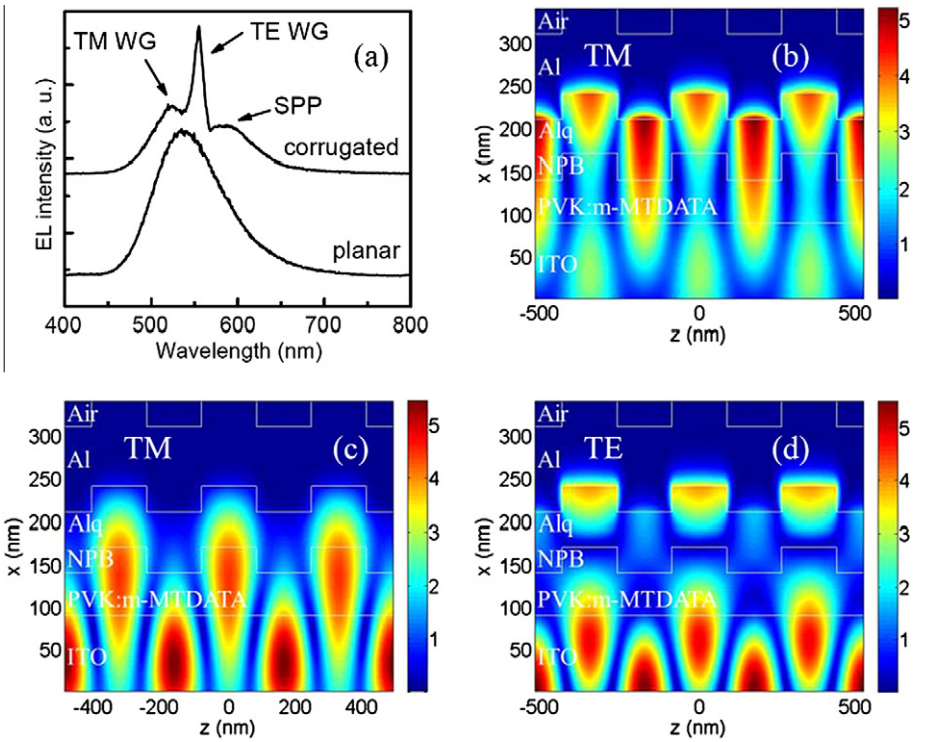

Fig. 6. EL spectra from both corrugated OLED with 350-nm grating and planar devices at normal direction (a), and distribution of the magnetic field intensity in the corrugated OLEDs at the wavelength of incident polarized light of 595 nm (b), 547 nm (c) and 520 nm (d), respectively.

the normal incident light is calculated to identify the optical modes for the devices with 350 nm grating period. Fig. 6 shows the field distribution at the illumination wavelength of 595, 547 and 520 nm, respectively, which corresponds to the three peak wavelength of the EL emission at normal direction. The field intensity is with maximum at the Al/Alq_3 interface and decay along the direction perpendicular to it at the wavelength of 595 nm

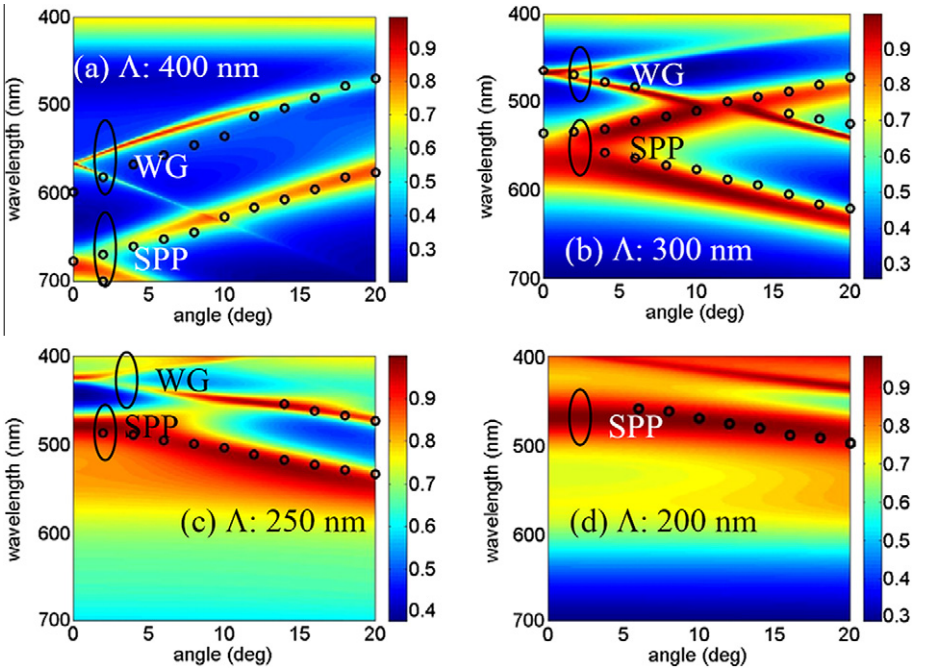

Fig. 7. Wavelength versus incident angle for the calculated dispersion relation of the corrugated OLEDs with various grating period (Λ) and for TM polarization. The measured dispersion relation extracted from the EL spectra (circles) is also shown.

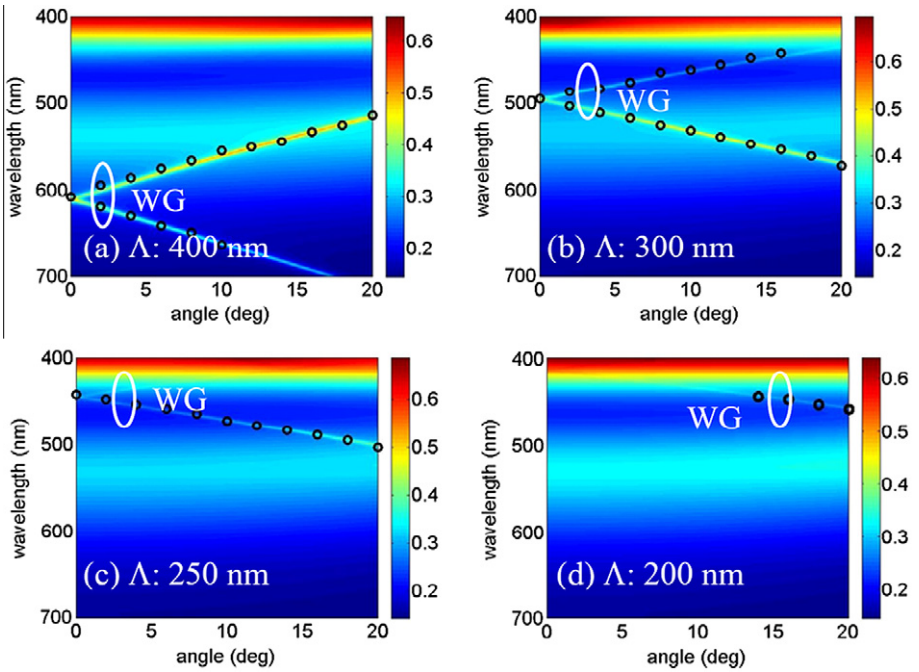

Fig. 8. Wavelength versus incident angle for the calculated dispersion relation of the corrugated OLEDs with various grating period and for TE polarization. The measured dispersion relation extracted from the EL spectra (circles) is also shown.

as shown in Fig. 6(b). We can conclude from this field distribution that the emission peak at 595 nm originates from SPP modes, since SPPs are surface wave and propagating along an interface between a metal and dielectric [42–46]. On the other hand, the field at the wavelength of 547 and 520 nm is mainly confined within the ITO and organic layers (Fig. 6(c) and (d)), which should be assigned to the TM and TE polarized WG modes due to the high refractive index of ITO and organic layers. Therefore the additional peaks shown in the EL spectra in Fig. 6(a) is identified as the SPP mode associated with the Al cathode/organic interface, and WG mode confined within the ITO and organic layers, respectively. This conclusion is applicable to the corrugated OLEDs with the various periods, except that the peak wavelength corresponding to the SPP and WG modes is shift with the different period, which has been verified by the following simulations.

The dispersion map derived from the simulated absorption spectra for the corrugated device with 400, 300, 250 and 200 nm grating period and for both TM and TE polarization is shown in Figs. 7 and 8, respectively, which also show agreement with the experimentally measurement extracted from the EL spectra. The extracted light emission from both the SPP and WG modes show blueshift with the decreasing of the grating period. Comparing the EL spectra from the corrugated and flat OLEDs at the normal direction (Fig. 4(f)), we can see that both the extracted SPP and WG modes located within the emission wavelength region of the Alq_3 emission for the device with the 350 nm grating period at the normal direction, which contribute to a more efficient outcoupling of the optical modes trapped in the devices and result in the highest EL efficiency for this OLED. Both the TM and TE polarized WG modes move out of the emission region of Alq_3 in case of the 200 and 250 nm grating period, while the emission band from the SPP mode becomes flat, which results in a smaller shift of the EL spectra at different observation angle and has been verified in Fig. 4(d) and (e). Therefore an improved viewing characteristic is expected. Our experimental and simulated data indicate that the power lost to both SPP and WG modes has been successfully recovered as light in far field for the corrugated OLEDs, which contributes to a much enhanced light extraction. It is possible to obtain a further improved light outcoupling by employing a 2-D grating due to its higher efficiency in coupling SPPs to far-filed radiation [47]. 2-D grating on the PVK:*m*-MTDATA by laser ablation has been realized (Fig. 1(e)), and further investigation are needed to explore its effect on the light outcoupling.

5. Conclusions

A periodic wavelength-scale corrugation has been introduced into OLEDs by one-step laser ablation of two interference beams, and enhanced outcoupling of radiation has been demonstrated. The introduction of this microstructure has allowed the observation of the emission originating from the SPP and WG modes, which are usually trapped within planar devices. An enhanced EL efficiency from the corrugated OLEDs has been observed. The microstructure has been directly formed on the HTL of the OLEDs by laser ablation without degradation of the device performance. While combining with the two-beam interference, both the period and the groove depth of the grating can be easily and precisely controlled, so that it is applicable to

OLEDs with different emission wavelength. With beam expansion, an entire wafer could be structured with one-shot nanosecond laser ablation, implying a broad industrial application prospect of the one-step efficient large-area approaches for OLEDs with much enhanced light outcoupling efficiency.

Acknowledgments

The authors gratefully acknowledge support from 973 Project (Grant Nos. 2010CB327701 and 2011CB013005), NSFC (Grant Nos. 60977025, 61177024 and 90923037) and NCET (Grant No. 070354).

References

[1] T. Chiba, Y.J. Pu, R. Miyazaki, K. Nakayama, H. Sasabe, J. Kido, Org. Electron. 12 (2011) 710–715.
[2] Y. Yang, T. Peng, K. Ye, Y. Wu, Y. Liu, Y. Wang, Org. Electron. 12 (2011) 29–33.
[3] L.H. Smith, A.E. Wasey, I.D.W. Samuel, W.L. Barnes, Adv. Funct. Mater. 15 (2005) 1839–1844.
[4] P.A. Hobson, S. Wedge, J.A.E. Wasey, I. Sage, W.L. Barnes, Adv. Mater. 14 (2002) 1393–1396.
[5] G. Gu, D.Z. Garbuzov, P.E. Burrows, S. Venkatesh, S.R. Forrest, M.E. Thompson, Opt. Lett. 22 (1997) 396–398.
[6] D.H. Kim, C.O. Cho, Y.G. Roh, H. Jeon, Y.S. Park, J. Cho, J.S. Im, C. Sone, Y. Park, W.J. Choi, Q.H. Park, Appl. Phys. Lett. 87 (2005) 203508.
[7] A.A. Erchak, D.J. Ripin, S. Fan, P. Rakich, J.D. Joannopoulos, E.P. Ippen, G.S. Petrich, L.A. Kolodziejski, Appl. Phys. Lett. 78 (2001) 563–565.
[8] T. Tsutsui, M. Yahiro, H. Yokogawa, K. Kawano, M. Yokoyama, Adv. Mater. 13 (2001) 1149–1152.
[9] S. Möller, S.R. Forrest, J. Appl. Phys. 91 (2002) 3324–3327.
[10] Y. Sun, S.R. Forrest, Nat. Photon. 2 (2008) 483–487.
[11] F. Li, X. Li, J. Zhang, B. Yang, Org. Electron. 8 (2007) 635–639.
[12] Y.R. Do, Y.C. Kim, Y.W. Song, C.O. Cho, H. Jeon, Y.J. Lee, S.H. Kim, Y.H. Lee, Adv. Mater. 15 (2003) 1214–1218.
[13] B.J. Matterson, J.M. Lupton, A.F. Safonov, M.G. Salt, W.L. Barnes, I.D.W. Samuel, Adv. Mater. 13 (2001) 123–127.
[14] A.H. Stephen, J.A.E. Easey, I. Sage, W.L. Barnes, Adv. Mater. 14 (2002) 1393–1396.
[15] B.J. Eggleton, R.E. Slusher, C.M. de Sterke, P.A. Krug, J.E. Sipe, Phys. Rev. Lett. 76 (1996) 1627–1630.
[16] C. Kallinger, M. Hilmer, A. Haugeneder, M. Perner, W. Spirkl, U. Lemmer, J. Feldmann, U. Scherf, K. Müllen, A. Gombert, V. Wittwer, Adv. Mater. 10 (1998) 920–923.
[17] H.A. Atwater, A. Polman, Nat. Mater. 9 (2010) 205–213.
[18] T. Okamoto, F. H'Dhili, S. Kawata, Appl. Phys. Lett. 85 (2004) 3968–3970.
[19] E. Hwang, I.I. Smolyaninov, C.C. Davis, Nano Lett. 10 (2010) 813–820.
[20] S. Nien, N. Chiu, Y. Ho, J. Lee, C. Lin, K. Wu, C. Lee, J. Lin, M. Wei, T. Chiu, Appl. Phys. Lett. 94 (2009) 103304.
[21] C.C. Chang, Y.D. Sharma, Y.S. Kim, J.A. Bur, R.V. Shenoi, S. Krishna, D. Huang, S.Y. Lin, Nano Lett. 10 (2010) 1704–1709.
[22] J. Feng, T. Okamoto, S. Kawata, Opt. Lett. 30 (2005) 2302–2304.
[23] K. Hong, H.K. Yu, I. Lee, K. Kim, S. Kim, J.L. Lee, Adv. Mater. 22 (2010) 4890.
[24] W.H. Koo, S.M. Jeong, F. Araoka, K. Ishikawa, S. Nishimura, T. Toyooka, H. Takezoe, Nat. Photon. 4 (2010) 222–226.
[25] E. Kim, Y. Xia, X.M. Zhao, G.M. Whitesides, Adv. Mater. 9 (1997) 651–654.
[26] J.R. Lawrence, G.A. Turnbull, I.D.W. Samuel, Appl. Phys. Lett. 82 (2003) 4023–4025.
[27] C.J. Yates, I.D.W. Samuel, P.L. Burn, S. Wedge, W.L. Barnes, Appl. Phys. Lett. 88 (2006) 161105.
[28] J. Wang, X. Sun, L. Chen, S.Y. Chou, Appl. Phys. Lett. 75 (1999) 2767–2769.
[29] T. Höfler, M. Weinberger, K. Wolfgang, S. Rentenberger, A. Pogantsch, Adv. Funct. Mater. 16 (2006) 2369–2373.
[30] Y. Shirota, Y. Kuwabara, H. lnada, T. Wakimoto, H. Nakada, Y. Yonemoto, S. Kawami, K. lmai, Appl. Phys. Lett. 65 (1994) 807–809.
[31] E. Sutcliffe, R. Srinivasan, J. Appl. Phys. 60 (1986) 3315–3322.
[32] N. Bityurin, B.S. Luk'yanchuk, M.H. Hong, T.C. Chong, Chem. Rev. 103 (2003) 519–552.
[33] T.C. Chong, M.H. Hong, L.P. Shi, Laser Photon. Rev. 4 (2010) 123–143.
[34] M. Prasad, P.F. Conforti, B.J. Garrison, J. Appl. Phys. 101 (2007) 103113.
[35] G. Bounos, A. Selimis, S. Georgiou, E. Rebollar, M. Castillejo, N. Bityurin, J. Appl. Phys. 100 (2006) 114323.
[36] B. Luk'yanchuk, N. Bityurin, S. Anisimov, A. Malyshev, N. Arnold, D. Bäuerle, Appl. Surf. Sci. 106 (1996) 120–125.
[37] D.Y. Kim, S.K. Tripathy, L. Li, J. Kumar, Appl. Phys. Lett. 66 (1995) 1166–1168.
[38] T. Lippert, T. Gerber, A. Wokaun, D.J. Funk, H. Fukumura, M. Goto, Appl. Phys. Lett. 75 (1999) 1018–1020.
[39] F. Yu, P. Li, H. Shen, S. Mathur, C.M. Lehr, U. Bakowsky, F. Mücklich, Biomaterials 26 (2005) 2307–2312.
[40] L.D. Merkle, M. Bass, R.T. Swimm, Opt. Eng. 22 (1983) 405–410.
[41] R.C. Hall, R. Mittra, K.M. Mitzner, IEEE T. Antenn. Propag. 36 (1988) 511.
[42] W.L. Barnes, A. Dereux, T.W. Ebbesen, Nature 424 (2003) 824–830.
[43] D. Oosten, M. Spasenović, L. Kuipers, Nano Lett. 10 (2010) 286–290.
[44] H. Gao, J. Henzie, T.W. Odom, Nano Lett. 6 (2006) 2104–2108.
[45] W.C. Liu, D.P. Tsai, Phys. Rev. B 65 (2002) 155423.
[46] J. Li, C.Z. Ning, Phys. Rev. Lett. 93 (2004) 087402.
[47] P.T. Worthing, W.L. Barnes, Appl. Phys. Lett. 79 (2001) 3035–3037.